

**Electronic reconstruction at *n*-type SrTiO<sub>3</sub>/LaAlO<sub>3</sub> interfaces**J. Verbeeck,<sup>1,\*</sup> S. Bals,<sup>1</sup> A. N. Kravtsova,<sup>1,†</sup> D. Lamoen,<sup>1</sup> M. Luysberg,<sup>2</sup> M. Huijben,<sup>3</sup> G. Rijnders,<sup>3</sup> A. Brinkman,<sup>3</sup> H. Hilgenkamp,<sup>3</sup> D. H. A. Blank,<sup>3</sup> and G. Van Tendeloo<sup>1</sup><sup>1</sup>EMAT, University of Antwerp, Groenenborgerlaan 171, 2020 Antwerp, Belgium<sup>2</sup>Institute of Solid State Research and Ernst Ruska Center for Microscopy and Spectroscopy with Electrons, Helmholtz Research Center–Jülich, 52425 Jülich, Germany<sup>3</sup>Faculty of Science and Technology and MESA + Institute for Nanotechnology, University of Twente, P.O. Box 217, 7500 AE Enschede, The Netherlands

(Received 14 January 2010; published 18 February 2010)

Electron-energy-loss spectroscopy (EELS) is used to investigate single layers of LaAlO<sub>3</sub> grown on SrTiO<sub>3</sub> having an *n*-type interface as well as multilayers of LaAlO<sub>3</sub> and SrTiO<sub>3</sub> in which both *n*- and *p*-type interfaces occur. Only minor changes in Ti valence at the *n*-type interface are observed. This finding seems to contradict earlier experiments for other SrTiO<sub>3</sub>/LaAlO<sub>3</sub> systems where large deviations in Ti valency were assumed to be responsible for the conductivity of these interfaces. *Ab initio* calculations have been carried out in order to interpret our EELS results. Using the concept of Bader charges, it is demonstrated that the so-called polar discontinuity is mainly resolved by lattice distortions and to a far lesser extent by changes in valency for both single layer and multilayer geometries.

DOI: [10.1103/PhysRevB.81.085113](https://doi.org/10.1103/PhysRevB.81.085113)

PACS number(s): 71.30.+h, 73.20.-r, 73.21.Ac, 79.20.Uv

**I. INTRODUCTION**

Interfaces between the insulating transition-metal oxides SrTiO<sub>3</sub> (STO) and LaAlO<sub>3</sub> (LAO) gained a lot of interest when it was found that for a specific stacking sequence of atomic planes at the interface, a conductive quasi-two-dimensional (2D) electron gas exists at the interface.<sup>1,2</sup> When LAO is grown on TiO<sub>2</sub>-terminated STO, a conducting interface (*n*-type) is obtained, whereas an insulating interface is found when growing LAO onto a SrO-terminated STO substrate (*p*-type).<sup>1,2</sup> Soon after, this experimental measurement was explained by an electronic reconstruction model<sup>3</sup> based on the fact that the atomic planes in STO are nominally charge neutral, whereas in LAO, the charge states are (LaO)<sup>+</sup> and (AlO<sub>2</sub>)<sup>-</sup> in principle. Therefore, a polar discontinuity is expected at the interface between STO and LAO. In order to stabilize this discontinuity, it has been suggested that an extra  $1/2e^-$  per interface unit cell is transferred from LAO to STO at the conducting interface, yielding a reduction of the valence for Ti from 4<sup>+</sup> to 3.5<sup>+</sup>. This model was supported by electron-energy-loss spectroscopy (EELS) measurements which showed the appearance of a valency change of Ti near the *n*-type interface spread out over a few nanometers.<sup>3</sup>

However, it became clear that the simple electronic structure model could not explain *all* the experimental details; researchers started investigating the role of oxygen vacancies,<sup>4,5</sup> chemical intermixing,<sup>4</sup> and lattice strain.<sup>6</sup> A wide range of interesting transport properties was measured,<sup>5,7–11</sup> and a broad overview of the structure-property relation of this system was published recently.<sup>12</sup>

Only a few experimental papers<sup>3,4,8,13</sup> investigated the microscopic origins of this conductive interface and especially EELS results have been scarce.<sup>3,4</sup> This is remarkable since EELS can, in principle, provide direct measurements of the electronic structure with atomic resolution and seems ideally suited for these heterostructures.

In this paper, we present experimental EELS results for both a single layer *n*-type interface sample as well as for a

multilayer sample<sup>7</sup> containing *n*- and *p*-type interfaces. Based on these measurements, we obtain an estimate for the Ti valency near the interface which we will compare with *ab initio* electronic structure calculations in order to obtain more insight on the role of the electronic reconstruction at these interfaces.

Many *ab initio* studies have been published on this subject already;<sup>6,14–17</sup> here we obtain estimates of the Ti valency by making use of the concept of Bader charges which can be directly compared to our experimental data. This calculation also provides insight in the role of electronic reconstruction, lattice deformation, and layer thickness in these systems. The fact that we, experimentally and theoretically, study both a single layer containing only an *n*-type interface and a multilayer containing both *n*- and *p*-type interfaces has the advantage that the differences between these different geometries can be explored.

**II. EXPERIMENTAL DETAILS AND RESULTS**

A single *n*-type interface sample was grown by depositing 20 nm of LAO on TiO<sub>2</sub> terminated STO by pulsed laser deposition at 850 °C and a O<sub>2</sub> pressure of 10<sup>-3</sup> mbar. A multilayer sample is grown under identical conditions as a repeated sequence of ten unit cells of LAO followed by ten unit cells of STO.

High angle annular dark field (HAADF) images as well as EELS spectra are acquired using a probe-corrected Titan 80–300 (FEI) in scanning transmission electron microscopy (STEM) mode. For EELS measurements, an effective probe size of  $\approx 5$  Å is used, taking beam broadening into account.<sup>30</sup> Spectra are recorded simultaneously from the low angle part of the scattering by using a Gatan GIF Tridiem with 2K charge coupled device camera having a collection and convergence angle  $\alpha = \beta = 25$  mrad. The energy resolution in EELS was approximately 0.5 eV.

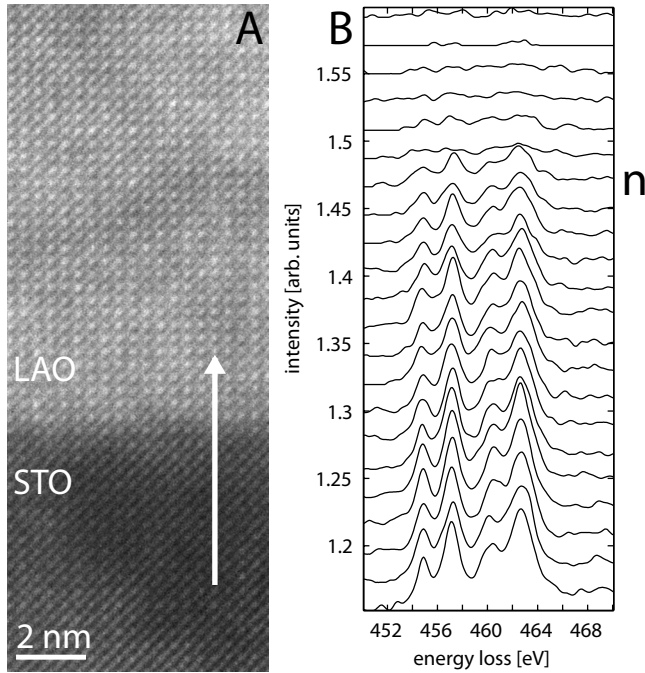


FIG. 1. (A) HAADF-STEM image of the single  $n$ -interface sample. (B) EELS  $\text{Ti-L}_{2,3}$  spectra across the interface from STO to LAO obtained along the direction indicated by the arrow in A. The approximate position of the  $n$ -type interface is indicated.

### EELS results

The structure of the single  $n$ -type interface sample is illustrated in Fig. 1(A) where a HAADF-STEM image is presented, showing a sharp interface between STO and LAO.

Figure 1(B) shows the  $\text{Ti-L}_{2,3}$  edge, taken along the arrow in Fig. 1(A). No remarkable difference is found between spectra obtained well within the substrate and those acquired closer to the interface. It must be noted that there is an abrupt disappearance of the Ti signal at the STO/LAO transition. This is in good agreement with the sharp interface as observed in the HAADF-STEM image.

The HAADF-STEM image of the multilayer sample is shown in Fig. 2(A), which is obtained with the same analytical probe as used for EELS. From this image, the sequence of ten unit cells of LAO and ten unit cells of STO can be confirmed. The white arrow indicates the direction and location of the EELS scan presented in Fig. 2(B). Since a  $\text{TiO}_2$ -terminated STO substrate was used for growth, the first interface along the growth direction is expected to be an  $n$ -type interface followed by a  $p$ -type interface. The EELS spectra show no indication toward a large deviation of the Ti valency at the interface.

Subtle changes in the fine structure of the  $\text{Ti-L}_{2,3}$  edge are often interpreted as indicators toward a variation in Ti valency.<sup>3,4</sup> We will therefore study the fine structure of the  $\text{Ti-L}_{2,3}$  edge in more detail in Fig. 3.<sup>31</sup> The  $\text{Ti-L}_{2,3}$  edge consists of four peaks, labeled a, b, c, and d. These peaks can be attributed to transitions from Ti  $2p$  to Ti  $3d$  levels with (a)  $2p_{3/2} \rightarrow 3d_{12_g}$ , (b)  $2p_{3/2} \rightarrow 3d_{e_g}$ , (c)  $2p_{1/2} \rightarrow 3d_{12_g}$ , and (d)  $2p_{1/2} \rightarrow 3d_{e_g}$ .<sup>4</sup>

For the  $n$ -type interface in the single layer sample, presented in Fig. 3(A), we note only small changes of the

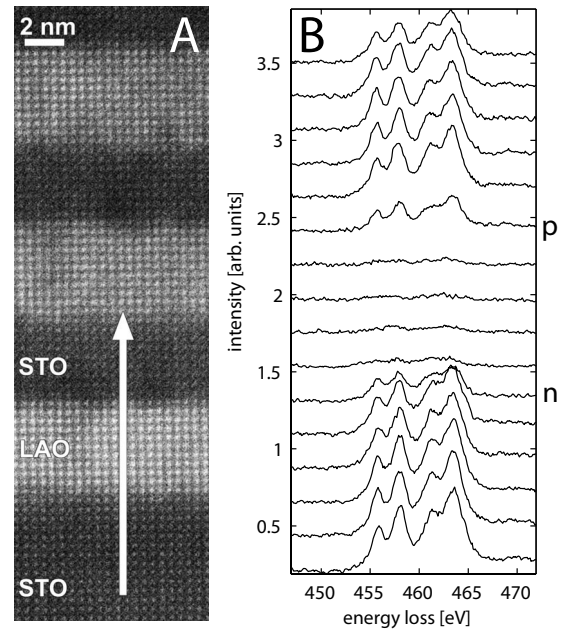


FIG. 2. (A) HAADF-STEM image of the multilayer sample acquired using the analytical probe which was used for the EELS measurements shown in B. The interfaces appear quite sharp although they tend to get rougher as the thickness of the sample increases along the direction of growth. (B) EELS  $\text{Ti-L}_{2,3}$  spectra across the first LAO layer obtained along the direction indicated by the arrow in A. The approximate position of  $n$ - and  $p$ -type interface is indicated.

$\text{Ti-L}_{2,3}$  edge near the interface indicating the absence of strong valency effects in this sample. Also for the multilayer sample represented in Fig. 3(B), only small changes in the  $\text{Ti-L}_{2,3}$  edge are present when comparing bulk STO with the  $n$ - and  $p$ -type interfaces. If we compare the spectra of the single  $n$ -type interface with the  $n$ -type interface in the multilayer sample, we note that in both cases there are only very small changes in the shape of these spectra with respect to the substrate, indicating a Ti environment very close to that of bulk STO.

Quantifying these differences in terms of valency changes is not straightforward since the exact shape of the edge depends not only on the valency but also on changes in the crystal structure. In addition, both effects are strongly coupled. Moreover, there are currently no commonly available *ab initio* electronic structure calculations that can accurately predict the detailed shape of this excitation edge which was shown to depend in a sensitive way on many-body excitation effects. Atomic multiplet approaches were more successful, but they require the input of crystal symmetry and crystal-field strength which are generally unknown.<sup>18,19</sup>

Keeping these difficulties in mind we have to resort to more qualitative fingerprinting techniques by comparing our  $\text{Ti-L}_{2,3}$  EELS edges with x-ray absorption spectroscopy (XAS) spectra obtained for  $\text{La}_{1-x}\text{Sr}_x\text{TiO}_3$  from Abbate *et al.*<sup>18</sup> reproduced in Fig. 3(C). It is important to note that the XAS data were obtained with an energy resolution of 90 meV whereas the EELS results have an energy resolution of approximately 0.5 eV. The effect of this resolution reduction

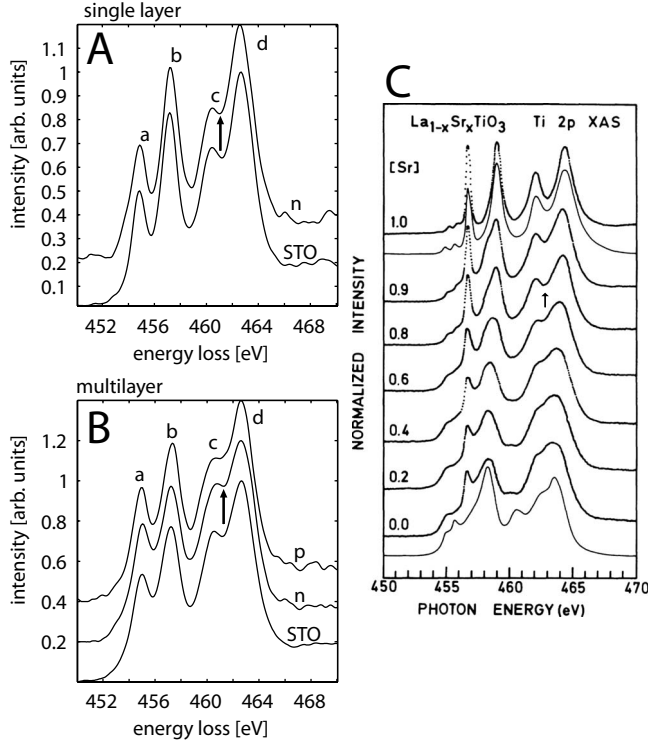


FIG. 3. Comparison between the Ti- $L_{2,3}$  spectra at the interface (*n* or *p*) and in the substrate (STO). (A) single *n*-type interface sample, (B) Multilayer sample containing both *n*- and *p*-type interfaces. (C) XAS reference spectra of  $\text{La}_{1-x}\text{Sr}_x\text{TiO}_3$  taken from Abate *et al.* (Ref. 18).

will be that the difference between the observed peak maxima and the minima between the peaks will be somewhat reduced in EELS as compared to the XAS data which complicates the comparison even further. Nevertheless, we can use the XAS reference data to estimate a lower boundary for the valency by comparing the shape of the Ti- $L_{2,3}$  edge between peaks *c* and *d* (indicated by an arrow). In Fig. 3(A), a clear valley is seen between peaks *c* and *d* for the STO substrate which is slightly reduced for the interface spectrum. The appearance of this valley is also seen in the XAS reference spectra, and the depth of this valley reduces up to  $x=0.8$  after which it becomes filled. We can use this observation to estimate the Ti valency from the EELS spectra to be at least  $\text{Ti}^{>3.8+}$  ( $x \geq 0.8$ ). It is important to point out that this is a *lower* boundary because the limited energy resolution in EELS will lead to a reduced contrast of the peaks and valleys in the spectrum as compared to the XAS results. For the multilayer sample, the same approach leads to an estimate of  $\text{Ti}^{>3.8+}$  for the *n*-type interface. Note that the *p*-type interface remarkably shows a bigger change in Ti- $L_{2,3}$  fine structure which could be due to the effect of oxygen vacancies near this interface. This finding again stresses the need for further advances in *ab initio* calculations.

### III. AB INITIO DETAILS AND RESULTS

In order to get a better understanding of the origins of the experimentally obtained small valency change, we perform

*ab initio* density-functional calculations. The density-functional theory formalism using the (linearized augmented planewave) (L)APW+lo method as implemented in the WIEN2K code<sup>20</sup> is used. In all our calculations we used muffin-tin radii of 2.0, 1.67, 1.75, 2.1, and 1.73 Bohr radii for Sr, O, Ti, La, and Al, respectively. The largest reciprocal-lattice vector  $K_{\text{max}}$  used in the plane-wave expansion was given by  $R_{\text{MT}}^{\text{min}} K_{\text{max}} = 5$ , where  $R_{\text{MT}}^{\text{min}}$  is the smallest muffin-tin radius. The Brillouin-zone integration was performed using 21 k-points in the irreducible wedge of the first Brillouin zone. The exchange-correlation potential was described by the Perdew-Burke-Ernzerhof functional.<sup>21</sup>

The structures which have been used for calculations are based on the bulk parameters of STO and LAO. Cubic STO has a lattice parameter of 3.905 Å,<sup>22</sup> whereas the pseudocubic unit cell of rhombohedral LAO has a lattice parameter  $a=3.791$  Å.<sup>23</sup> In our calculations we assume that the LAO adopts the in-plane lattice parameter of the STO (001) substrate  $a=b=3.905$  Å. This in-plane tensile strain causes a decrease of the lattice parameter along the growth direction, which in principle can be determined from Poisson's ratio. A previous x-ray diffraction study of LAO films grown epitaxially onto a  $\text{TiO}_2$ -terminated (100) surface of STO (Ref. 12) has shown that the lattice parameter of LAO along the growth direction was 3.73 Å, which corresponds to a 1.6% decrease as compared to the bulk lattice parameter of LAO, consistent with TEM exit-wave experiments on the same specimen.

In our calculations, different stackings have been built, containing an equal amount of STO and LAO unit cells (2+2, 4+4, 8+8). These systems have been calculated with periodic boundary conditions. This implies that both types of interface are present. Besides these structures, a multilayer yielding only *n*-type interfaces is calculated by constructing a (8.5+7.5) geometry. Furthermore, a single LAO layer on STO is simulated by including a vacuum region above the last LAO atomic plane (8+8+vac.) similar to the structure calculated in.<sup>6</sup> In the latter configuration, only one *n*-type interface is present and this geometry is in closest agreement to the experimental single interface sample. The geometry of the (8+8) system on the other hand, is in closest agreement to our experimental multilayer sample, where a repeated stacking of ten unit cells of STO and ten unit cells of LAO is present.

Atomic positions have been relaxed for all systems by minimizing the forces on the atoms. The forces driving the relaxation are mainly due to the polar character of the LAO system. Indeed, the dipole created by the polar discontinuity at the *p*- and/or *n*-type interface can be compensated by a reorganization of the electrons (such as proposed by Ref. 3) but *also* by a displacement of the atoms, as was shown to be important in Ref. 6. It should be noted that here, both mechanisms are taken into account.

All atomic displacements are in the pm range [ $\leq 8.8$  pm for (4+4),  $\leq 8.2$  pm for (8+8), and  $\leq 11$  pm for (8+8+vac.)]. For all systems a polar distortion is found whereby a displacement of the cations with respect to the oxygen octahedra creates a ferroelectric field that compensates the polar discontinuity near the *p*- or *n*-type interface. This polar distortion is in agreement with previous results in systems



TABLE I. Bader analysis and extrapolated valences for different geometries. All geometries are relaxed.

System	Band gap (eV)	Ti center ( <i>e</i> )	Ti interface ( <i>e</i> )	Ti valence interface
(2+2)	1.8	2.53	2.55	4.00 <sup>+</sup>
(4+4)	1.1	2.53	2.55	4.00 <sup>+</sup>
(8+8)	0	2.53	2.54	3.97 <sup>+</sup>
(8.5+7.5)	0	2.54	2.45	3.74 <sup>+</sup>
(8+8+vac.)	0	2.55	2.50	3.87 <sup>+</sup>

where only *n*-type interfaces are present.<sup>6,24–26</sup>

To investigate the electronic properties of the STO/LAO multilayer as a function of layer thickness, the density of states (DOS) has been calculated. The derived band gap *after* structural relaxation is listed in Table I for all geometries. We observe a decrease in band gap as the layer thickness increases with a closing of the band gap for the (8+8) system. These results follow the same trend as what was observed for trilayer structures containing both a *p*- and a *n*-type interface. In such systems a drastic increase in the sheet resistance was found to occur below a critical layer thickness of approximately six unit cells.<sup>7</sup>

In order to understand our experimental findings concerning the Ti valence, the atomic charge assigned to Ti by the so-called atoms-in-molecules approach of Bader<sup>27</sup> has been computed. In bulk STO, the atomic charge of Ti equals 2.55*e* while for bulk LaTiO<sub>3</sub> a charge of 2.16*e* is found for Ti.<sup>32</sup> Associating the STO and LTO bulk values with their nominal Ti<sup>4+</sup> and Ti<sup>3+</sup> valence, we can estimate the Ti valence at the *n*-type interface in Table I.

It can be seen that the valence of the Ti ion at the interface tends to 4<sup>+</sup> for all relaxed multilayer geometries containing *n*- and *p*-type interfaces. For geometries where metallic conduction is found, a slight reduction in the Ti valence at the interface is observed. From this analysis we can expect the nominal Ti valence at the interface in our experimental multilayer sample [which would correspond to a (10+10) stacking] to be slightly different from Ti<sup>4+</sup> in agreement with our observations. In any case, the calculated valency changes are much smaller than what is expected when assuming only electronic compensation of the polar discontinuity as in (Ref. 3).

For systems containing one or more *n*-type interfaces only ((8.5+7.5) and (8+8+vac.)), a larger deviation with respect to Ti<sup>4+</sup> is found although the calculated valency for the (8+8+vac.) is still rather close to 4<sup>+</sup>. This difference between multilayers containing both *n*- and *p*-type interface and geometries containing only *n*-type interfaces could be related to the creation of a dipole field in multilayers with *n*- and *p*-type interfaces, which is absent in layers where only *n*-type interfaces are present. Due to the difficulties when quantifying valency changes from EELS spectra, as described above, this subtle difference could not directly be resolved in our experiments. However our experiments do not contradict the theoretical predictions either since a *lower* boundary of Ti<sup>>3.8</sup> was found in each case.

The results for the single layer of LAO with vacuum (8+8+vac.) show a similarly large effect of lattice relaxation

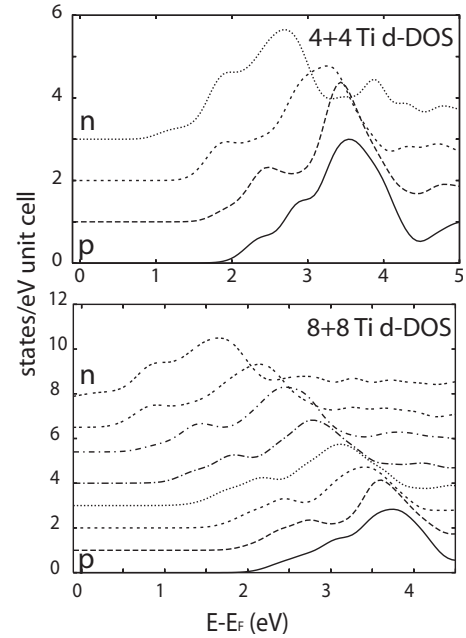


FIG. 4. Unoccupied Ti *d* DOS calculations for the (4+4) and the (8+8) system. For each type, *n*-type and *p*-type interfaces are indicated. Note the presence of a band gap for the (4+4) case while for (8+8) the interface remains metallic and a small Ti valency change is expected. Each layer is offset by 1 for better visibility.

on the electronic structure as already observed by Pentcheva *et al.*<sup>6</sup> This polar distortion reduces strongly the need for electronic screening of the polar discontinuity and therefore the predicted valency of 3.87<sup>+</sup> is rather close to 4<sup>+</sup> in agreement with our experimental lower bound of Ti<sup>>3.8+</sup> and with the experimental estimate of Salluzo *et al.* of Ti<sup>3.9+</sup> (Ref. 13) and of Thiel *et al.* of Ti<sup>3.97</sup>.<sup>8</sup> Earlier work by Nakagawa *et al.*<sup>3</sup> showed a much lower estimate of Ti<sup>3.3+</sup> which may be due to differences in growth and possible occurrence of oxygen vacancies.<sup>4,8</sup>

In order to get more insight in the details of the electronic behavior of the 4+4 and 8+8 multilayers, the projected DOS for the Ti *d* band is shown in Fig. 4 for the unoccupied states comparable to the work of Son *et al.*<sup>15</sup> for single layers. For simplicity, only the (4+4) and the (8+8) systems are shown. For the (4+4) system a band gap is observed while for the (8+8) system the Ti *d* band slightly crosses the Fermi level at the *n* interface. It must be noted however that the amount of *d* electrons below the Fermi level is very small in agreement with the fact that according to the Bader analysis the Ti valence remains close to 4<sup>+</sup>.

From Fig. 4 it is furthermore clearer that there is a shift in the maximum of the Ti *d*-DOS (in case of the 8+8 system ≈2 eV) across the layers. This effect is in excellent agreement with the calculation of Bristowe *et al.*<sup>16</sup> who explained the insulator metal transition as caused by the crossing of the band gap due to a constant electrostatic field between *n*- and *p*-interfaces. This field is constant up to the point where the layer thickness would make the accumulated shift in the DOS cross the Fermi level. In our case these fields can be estimated as approximately 0.25 eV/unit cell (4+4 and 8+8) in excellent agreement with Ref. 16. This shift in the *d*

DOS does not lead to a shift in the EELS excitation edges because calculations of the Ti 2*p* core states show a similar shift resulting in a strongly reduced excitation energy *difference* across the layers of less than 60 meV, difficult to observe by EELS. The shift of the Ti *d* band however seems to be of fundamental importance to understand the behavior of these layers and a potential technique to measure this shift might be electron holography.<sup>28</sup>

#### IV. DISCUSSION

From the EELS experiments we were able to estimate a lower boundary for the valency change to Ti<sup>>3.8+</sup> for *n*-type interfaces in both single and multilayer samples. This is somewhat surprising since much lower experimental estimates even below Ti<sup>3.5+</sup> were found<sup>3,29</sup> on similar samples. A possible explanation for this discrepancy could be the different growth conditions for the samples, but practically the same results for completely different oxygen partial pressures during the growth ( $8 \times 10^{-5}$  and  $2 \times 10^{-3}$  mbar) were obtained by Salluzzo *et al.*<sup>13</sup>

On the other hand, our experimental findings are in agreement with recent observation of Salluzzo *et al.* where depth resolved XAS was used to estimate the valency in single *n*-type interface LAO layers to be at least Ti<sup>3.9+</sup>. It has to be noted however that EELS has an intrinsic better *spatial* resolution as compared to depth resolved XAS as in Ref. 13.

Our experimental findings are also in agreement with our DFT estimates of the charge on Ti being very close to 4+ for both the single layer geometry (8+8+vac.) as well as for the multilayer geometry (8+8). It is important to note however that the conduction in both single layer and multilayers is due to electrons with Ti *d* character although their density is considerably less than what would be expected from a simple ionic model.

These small valency changes also raise questions about the purely ionic polar discontinuity model.<sup>3</sup> Indeed, our DFT calculations also give insight in the crucial effect of strain on the electronic structure. Although the atomic displacements are small, the structural displacements compensate to a large extent the polar discontinuity near the LAO interface and this

effect is somewhat different in geometries containing both *n*- and *p*-interfaces and those only containing *n*-interfaces. These observations are in favor of a model where ferroelectric distortions are in competition with electronic compensation of the uncompensated charges from LAO near the interfaces.<sup>6</sup>

It is important to note here that vacancies in these samples are unlikely to be present in view of the high oxygen pressure of  $10^{-3}$  mbar used during growth. Also, chemical intermixing near the interface seems to be very limited as can be observed from the sharpness of the Ti signal when scanned over the interfaces in Figs. 1(B) and 2(B). An estimate of the upper boundary for Ti interdiffusion can be made to approximately one unit cell, especially when the spatial resolution effect of the microscope is taken into account.

#### V. CONCLUSION

In conclusion, single layers containing only one *n*-type interface and multilayers of STO and LAO in which both the *n*- and *p*-type interfaces are present have been investigated by experimental EELS and HAADF-STEM. By comparing to XAS measurements a lower boundary of Ti<sup>>3.8+</sup> is found at the *n*-type interface in single layers as well as multilayer samples.

These changes are smaller than those expected in the ionic polar discontinuity model. Combining our experimental findings with our theoretical results indicates that the polar discontinuity is compensated in the first place by lattice distortions and only in second order by electronic compensation. As a consequence, the Ti valence at the interface stays close to a value of 4<sup>+</sup>.

#### ACKNOWLEDGMENTS

The authors acknowledge financial support from the European Union under the Framework 6 program under a contract for an Integrated Infrastructure Initiative (Reference No. 026019 ESTEEM). S.B. gratefully acknowledges financial support from the FWO-Vlaanderen. C. Mitterbauer of FEI is acknowledged for recording the experimental data on the single interface sample during a demonstration session on the FEI Titan 80-300 microscope.

\*jo.verbeeck@ua.ac.be

<sup>†</sup>Present address: Faculty of Physics, Southern Federal University, Sorge 5, Rostov-on-Don 344090, Russia.

<sup>1</sup>A. Ohtomo and H. Hwang, Nature (London) **427**, 423 (2004).

<sup>2</sup>A. Ohtomo and H. Y. Hwang, Nature (London) **441**, 120 (2006).

<sup>3</sup>N. Nakagawa, H. Y. Hwang, and D. Muller, Nature Mater. **5**, 204 (2006).

<sup>4</sup>J.-L. Maurice *et al.*, EPL **82**, 17003 (2008).

<sup>5</sup>A. Brinkman, M. Huijben, M. van Zalk, J. Huijben, U. Zeitler, J. C. Maan, W. G. van der Wiel, G. Rijnders, D. H. A. Blank, and H. Hilgenkamp, Nature Mater. **6**, 493 (2007).

<sup>6</sup>R. Pentcheva and W. E. Pickett, Phys. Rev. Lett. **102**, 107602 (2009).

<sup>7</sup>M. Huijben, G. Rijnders, D. H. A. Blank, S. Bals, S. V. Aert, J. Verbeeck, G. V. Tendeloo, A. Brinkman, and H. Hilgenkamp, Nature Mater. **5**, 556 (2006).

<sup>8</sup>S. Thiel, G. Hammert, A. Schmehl, C. Schneider, and J. Mannhart, Science **313**, 1942 (2006).

<sup>9</sup>N. Reyren *et al.*, Science **317**, 1196 (2007).

<sup>10</sup>A. D. Caviglia, S. Gariglio, N. Reyren, D. Jaccard, T. Schneider, M. Gabay, S. Thiel, G. Hammerl, J. Mannhart, and J.-M. Triscone, Nature (London) **456**, 624 (2008).

<sup>11</sup>M. Basletic, J.-L. Maurice, C. Carr  tero, G. Herranz, O. Copie, M. Bibes, E. Jacquet, K. Bouzehouane, S. Fusil, and A. Barth  l  my, Nature Mater. **7**, 621 (2008).

<sup>12</sup>M. Huijben, A. Brinkman, G. Koster, G. Rijnders, H. Hilgen-

- kamp, and D. H. A. Blank, *Adv. Mater.* **21**, 1665 (2009).
- <sup>13</sup>M. Salluzzo *et al.*, *Phys. Rev. Lett.* **102**, 166804 (2009).
- <sup>14</sup>M. S. Park, S. H. Rhim, and A. J. Freeman, *Phys. Rev. B* **74**, 205416 (2006).
- <sup>15</sup>W. J. Son, E. Cho, B. Lee, J. Lee, and S. Han, *Phys. Rev. B* **79**, 245411 (2009).
- <sup>16</sup>N. C. Bristowe, E. Artacho, and P. B. Littlewood, *Phys. Rev. B* **80**, 045425 (2009).
- <sup>17</sup>R. Pentcheva and W. E. Pickett, *Phys. Rev. B* **74**, 035112 (2006).
- <sup>18</sup>M. Abbate *et al.*, *Phys. Rev. B* **44**, 5419 (1991).
- <sup>19</sup>F. M. F. de Groot, J. C. Fuggle, B. T. Thole, and G. A. Sawatzky, *Phys. Rev. B* **41**, 928 (1990).
- <sup>20</sup>P. Blaha, K. Schwarz, G. K. H. Madsen, D. Kvasnicka, and J. Luitz, *WIEN2K, An Augmented Plane Wave+Local Orbitals Program for Calculating Crystal Properties* (Karlheinz Schwarz-Technische Universität Wien, Austria, Wien, 2001).
- <sup>21</sup>J. P. Perdew, K. Burke, and M. Ernzerhof, *Phys. Rev. Lett.* **77**, 3865 (1996).
- <sup>22</sup>Y. A. Abramov, V. G. Tsirelson, V. E. Zavodnik, S. A. Ivanov, and B. I. D., *Acta Crystallogr., Sect. B: Struct. Sci.* **51**, 942 (1995).
- <sup>23</sup>S. A. Hayward *et al.*, *Phys. Rev. B* **72**, 054110 (2005).
- <sup>24</sup>P. Willmott *et al.*, *Phys. Rev. Lett.* **99**, 155502 (2007).
- <sup>25</sup>V. Vonk, M. Huijben, K. J. I. Driessen, P. Tinnemans, A. Brinkman, S. Harkema, and H. Graafsma, *Phys. Rev. B* **75**, 235417 (2007).
- <sup>26</sup>Z. Zhong and P. J. Kelly, *EPL* **84**, 27001 (2008).
- <sup>27</sup>R. Bader, *Atoms in Molecules, A Quantum Theory* (Clarendon, New York, 1990).
- <sup>28</sup>H. Lichte and M. Lehmann, *Microsc. Microanal.* **9**, Suppl. S03, 14 (2003).
- <sup>29</sup>M. Sing *et al.*, *Phys. Rev. Lett.* **102**, 176805 (2009).
- <sup>30</sup>Beam broadening is often implicitly neglected but makes a significant contribution to the size of the STEM probe. Just noting the nominal beam diameter impinging on the sample leads to a serious under estimation of the actual spatial resolution in STEM EELS.
- <sup>31</sup>To obtain this figure, several data treatment steps were needed: a background extrapolation, cross correlation to remove energy drift, Gaussian smoothing with a FWHM=0.5 eV to improve the signal-to-noise ratio. For the single interface sample, the interface signal is taken as the sum of three spectra near the interface over a distance of 0.6 nm. For the multilayer sample, a sum of two spectra taken at the first and second *n*-type interface and at the first and second *p*-type interface is taken after checking that the trend in the first and second interface was identical.
- <sup>32</sup>We neglected electron correlation effects which lead to the Mott-insulating ground state of LaTiO<sub>3</sub>.